EUROPEAN COMMISSION
5th EURATOM FRAMEWORK PROGRAMME 1998-2002
KEY ACTION : NUCLEAR FISSION

HTR-M

European Project for the development of HTR Technology - Materials for the HTR

CONTRACT N°
FIKI-CT-2000-00032
&
FIKI-CT-2001-00135

Studies on Mechanical behaviour of Mod 9Cr 1Mo steel -
CEA R & D Programme
by

M.T.Cabrillat, (CEA Cadarache)
M. Reytier, M. Sauzay, M. Mottot, J. L. Seran, P.Billot (CEA Saclay)
V Gaffard, (Ecole de Mines)
B. Riou (Framatome.ANP)

France

Dissemination level : CO
Document Number: HTR-M-04/09-D-1.0.108

STUDIES ON MECHANICAL BEHAVIOR OF MOD 9CR-1MO STEEL. CEA R&D PROGRAM

Marie Therese Cabrillat, Magali Reytier*, Maxime Sauzay*, Michel Mottot*, Vincent Gaffard****, Jean Louis Seran*, Philippe Billot*, Bernard Riou*****
* CEA/DEN/Saclay, 91191 Gif-sur-Yvette, France
** CEA/DEN/Cadarache, 13108 Saint-Paul-lez-Durance, Cedex, France
***Framatome-ANP, 69456 Lyon Cedex 06, France
**** Ecole des Mines de Paris, Centre des Materiaux, BP 87, 91003 Evry Cedex, France

ABSTRACT: 9Cr-1Mo mod steel is one candidate material for the VHTR pressure vessel. Research programs have been undertaken at CEA to characterize the behavior of this steel and of its welded junctions in representative loading situations - fatigue, creep and creep-fatigue solicitations - with several objectives: definition and validation of design rules, characterization and validation of defect nocivity assessment methods, development of physically based behavior and damage models which can be used with confidence outside their identification domain, acquisition of missing data.

Experimental and numerical programs have been undertaken in several fields:

* Fatigue behavior in order to check if there is an influence of the mean stress on the fatigue life of the component and to propose design methods to take it into account if necessary.
* Creep behavior and creep damage of the base metal (BM) and of the weld junctions, in order to identify the weak zones in creep situations, to characterize the behavior and the damage laws of the different zones of the weld junctions, and to provide rules and material data for the life assessment methods.
* Cyclic behavior in the creep range in order to evaluate the influence of hold time on the fatigue life and to propose validated inelastic models based on the physical strain mechanisms.
* Characterization of fatigue and creep crack growth laws for base metal and weld metal, and realization of tests on large components with defects either in BM or in the weld in order to validate the assessment procedures for the residual life estimation of cracked components.

A description of these different programs is proposed, and the first results obtained are presented.

KEY WORDS: mod 9Cr-1Mo steel; VHTR pressure vessel; design rules; creep; creep-fatigue; defect nocivity assessment.

0. INTRODUCTION

In the framework of GEN IV studies, CEA is involved in many research activities concerning the development and the validation of materials suitable for GCR (Gas Cooled Reactors), either for GFR (Gas Cooled Fast Reactors) or for VHTR (Very High Temperature Reactors). The objective is to validate or develop materials able to withstand GCR conditions: environment (He atmosphere, irradiation level), pressure and temperature levels. Studies are in progress on different kinds of materials selected for the different structures, depending on the operating conditions. Mod 9Cr-1Mo steel is the candidate material for the RPV (Reactor Pressure Vessel) and for some internal components; other materials studied are: Ni-Base alloys and superalloys for structures working at intermediate temperatures (650-950°C), graphite, C/C composites and ceramics for higher temperatures [1].

This paper presents the research program undertaken at CEA on mod 9Cr-1Mo steel with the aim to improve the knowledge concerning the mechanical behavior for the base metal but also for the welded junctions. Several objectives are considered: validation and/or improvement of design rules, characterization and validation of defect nocivity assessment methods, development of physically based behavior and damage models which can be used with confidence outside their identification domain, acquisition of missing data. The following situations have to be investigated: fatigue, creep and creep-fatigue interaction. Complementary metallurgical studies are realized on this steel. The corresponding program and the first results are presented in [2].

1. OPERATING CONDITIONS FOR THE PRESSURE VESSEL

The RPV is a key component for the GCR. The planned operating conditions are the following ones:

- Coolant gas (He) pressure is up to 70 bar. Lower values should be expected for VHTR.
- The vessel temperature in nominal situations will be fixed in order to keep the structure in the negligible creep domain to avoid the development of a specific in-service surveillance program. Consequently, an important point is the determination of this negligible creep domain. For that, it will be also necessary to consider the temperatures reached during the transients in accidental conditions and the time spent at these temperatures. Due to that, creep resistance will be a key point for the validation of the vessel material selection.
- The vessel must be designed for a life duration of 60 years, with a loading rate of 80%, which leads to about 4.10^5 hours.
- The maximum expected fluence for the vessel is estimated to be about 8.10^{18} n/cm^2 (for neutrons with energy E>0.1 MeV) that is lower than the end-of-life doses of PWR (Pressure Water Reactors) vessels. Consequently, we can expect that such a low level of irradiation can induce only negligible effect on the mechanical properties and particularly in case of materials belonging to the class of high Cr martensitic steels. Specific programs are running in the framework of a European program to check this point [3].

The thickness of the RPV is a function of the internal pressure and of the temperature reached on the vessel. With the present operating conditions, its minimal value is about 180 mm. Due to this important thickness, difficulties can be expected for the fabrication. Specific studies are running to check the weldability in such conditions and to evaluate the variability of microstructures and consequently of mechanical properties in the thickness [4].

2. MECHANICAL DESIGN OF THE RPV

Different design codes can be used for RPV design, mainly ASME or RCC-MR. These two codes have been examined in order to assess their applicability to the design of the GCR RPV, and to identify the developments which are necessary. At the present time, data for mod 9Cr-1Mo steel are included in ASME code for temperatures lower than 371°C; no data are available in ASME Appendix NH for operation in the creep range, but work is in progress and there are plans to introduce it in future revisions. In the last RCC-MR issue [5], data for this steel have been updated. Nevertheless, it appears that it is necessary to validate or improve some design rules and to define complementary programs in order to get missing data. These programs are described in the following sections. In section 4, we present the studies on fatigue and creep behavior of the base metal and of the welded junctions. In section 5, we present the studies to validate the defect nocivity analyses and acquire the missing data.

3. STUDIES ON FATIGUE, CREEP AND CREEP-FATIGUE BEHAVIOR

a) Fatigue behavior

Because of the high static pressure applied inside some of the tubes and components, a static loading will be superimposed to the classical cyclic loading due to the in-service use of the reactor. It should be noticed that this high pressure would induce tensile stresses of about 100-150 MPa in such components. This mean stress value could be damaging because of ratcheting and/or because of fatigue crack initiation/propagation. In order to evaluate this mean stress effect, cyclic torsion tests have been carried out, with and without a superimposed static tensile stress.

The material of the study is a Z10CDVNb 9.1 martensitic steel whose chemical composition is shown in table 1. The plate has been heat treated (1050°C during 30min and then air cooled) and then tempered (780°C during one hour). Its thickness is 30 mm.

Table 1 : Chemical composition of the steel sheet

Elements	**C**	**Mn**	**P**	**S**	**Si**	**Cu**	**Ni**	**Cr**	**Mo**	**Al**	
% wt	0.086	0.363	0.017	0.0010	0.324	0.068	0.149	8.910	0.917	0.018	
Eléments	**Nb**	**V**	**N_2**	**Sn**	**Zr**	**Ti**	**As**	**W**	**B**	**Sb**	**O_2**
%wt	0.080	0.198	0.0411	0.005	0.001	0.002	0.0122	0.010	0.0010	0.0006	0.0018

Varied cyclic shear strain levels have been applied. Tests were conducted at 550°C. As a first approach, a tensile stress magnitude of 150 MPa has been chosen. The results of the experimental tests show clearly the effect of the mean stress. For high cyclic strain levels, the lifetime reduction factor with respect to the pure torsion test results is about 2-3 (Figure 1), but for such loading conditions (high stress levels), we can suspect that there is not only fatigue damage; complementary work will be necessary to check this point. For lower cyclic shear strain levels, the lifetime reduction factor increases when the applied cyclic strain decreases. When the number of cycles to failure without mean tensile stress is about 35000 cycles, the reduction factor is about 5-6 (Figure 1). The same trends have been observed for an austenitic stainless steel. It should be noticed that the in-service cyclic strain will be lower than the smaller strain which was applied during our tests. Therefore, complementary tests for a smaller applied cyclic shear strain are needed for evaluating the reduction factor due to the mean stress effect in the in-service conditions.

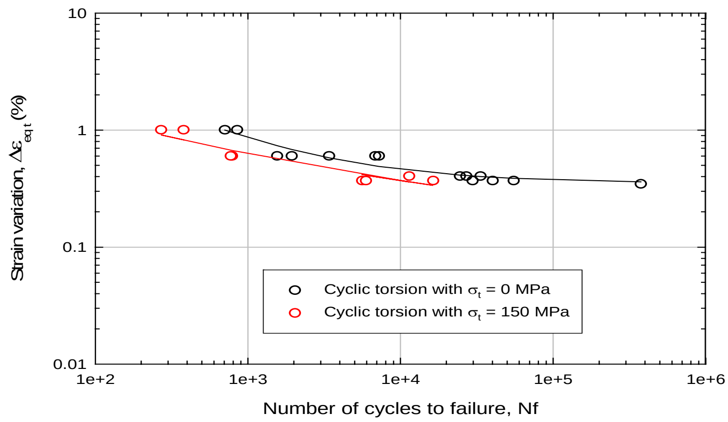

Figure 1: Effect of the tensile mean stress, σ_t, on the lifetime during cyclic torsion tests.

These tests are also used to study the ratcheting behavior of this steel. At 550°C, for a tensile stress equal to 150 MPa, this effect seems important: no saturation of the tensile strain is observed, even for the lowest shear strain value (ε_{eq} = ± 0.18%) for which a tensile strain about 4% was obtained at midlife. To supplement this study, complementary tests using a smaller tensile stress are scheduled, as well as tests at lower temperatures.

b) Creep behavior

i. Negligible creep domain

The determination of the negligible creep domain is a major point for the RPV design. For that purpose, it is necessary to have validated creep strain laws at low temperatures, typically in the range 400-500°C, but also at low stress levels corresponding to S_m or 1.5 S_m where S_m is the allowable stress at the temperature considered. The corresponding data are available in the RCC-MR [5], but for such loading conditions, these laws were obtained by extrapolating results at higher temperatures and higher stresses. Reference [6] presents creep strain laws for this steel and uses them to build isochronous curves which should be a basis for ASME. The comparison of these laws at low temperatures lead to different conclusions: following laws issued from [6], there will be no creep strain at 427°C for a stress level of 252 MPa (i.e. 1.5 S_m at this temperature) for 10^5 h (see figure 2) while using creep strain laws of RCC-MR, we predict a creep strain equal to 0.1% in 4000 h (figure 3).

It appears necessary to precise the real creep behavior of the steel in such temperature and loading conditions. A specific program is running at CEA for that purpose. Creep tests have been launched at low stress levels in the temperature range 400-500°C. Results will be available in a few months.

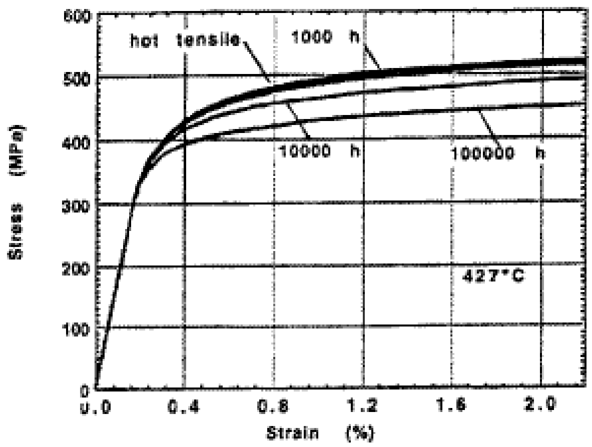

Fig. 2 : isochronous curves for mod 9Cr-1Mo at 427°C (from [6])

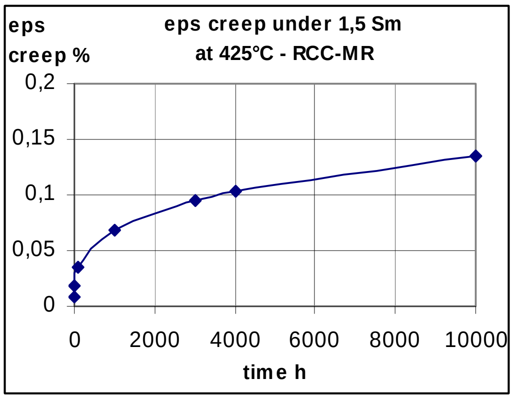

Fig. 3 : creep strain under 1.5 Sm at 425°C RCC-MR [5]

ii. Creep behavior and creep damage evaluation for base metal and welded junctions

In incidental and accidental situations, temperature will be increased and the RPV will stay in a creep-controlled condition for several hours. Weld joints, and specially HAZ (Heat Affected Zone), are the weak zones in creep situations. Type IV cracking is a typical failure which occurs in the intercritical zone, which is the part of the HAZ where the maximum temperature reached during the welding operation is in the range [A_{c1}, A_{c3}], A_{c1} being the temperature at which martensite to austenite transformation starts during heating, A_{c3} temperature at which it stops. This zone is close to the base metal and it presents a lower hardness and a lower rupture ductility than the other ones.

In order to predict the behavior and the life of structures, it is necessary to develop and validate creep behavior and creep damage models which can be used in a wide range of loading conditions. To reach this objective, the models have to be based on the physical mechanisms of deformation and of damage. As many other materials, mod 9Cr-1Mo exhibits a complex creep behavior with several creep flow regimes, typically a high stress deformation regime controlled by cross-slip or dislocation climb and a low stress deformation regime controlled by grain boundary diffusion.

Previous works on austenitic steels, which have been extensively studied, allowed developing and validating intergranular creep damage models considering contribution of cavity nucleation and of cavity growth by viscoplastic deformation of the matrix and by diffusion mechanism [7]. This approach allowed predicting very good results on uniaxial samples and on notched specimens when compared to experimental ones. Moreover, evaluation of creep crack initiation and growth from an initial defect on CT and axisymetric specimens leads to satisfactory results, in good agreement with experimental ones.

The same methodology is used for mod 9Cr-1Mo steel in the framework of a PhD program performed at Ecole des Mines de Paris with the contribution of Framatome-ANP, EDF and CEA. The material of the study is not the same as in the previous studies on fatigue behavior. It is a tempered chromium martensitic stainless steel whose chemical composition is given in table 2. It was supplied as a pipe of 295 mm in outer diameter and 55 mm in thickness. A lot of investigations have been performed:

- identification of the weak zone in uniaxial creep tests on samples with welds,
- metallurgical and mechanical characterizations of BM (Base Metal), WM (Weld Metal) and HAZ of real welds. Concerning HAZ, the intercritical zone is specially studied, as it is the weakest zone in creep situations. The characterizations are then used to realize "simulated HAZ" representative of this weakest part, in order to obtain enough material to perform creep tests on homogeneous samples representative of the HAZ. The simulated HAZ are obtained by applying appropriate thermomechanical loadings using a Gleeble machine,
- identification of creep damage mechanisms for BM and simulated HAZ,
- development of continuum damage models, based on these physical mechanisms,
- validation of these models.

Table 2: chemical composition of the material studied

Elements	**C**	**Si**	**Mn**	**P**	**S**	**Al**	**Cr**	**Ni**	**Mo**	**V**	**Nb**	**N**
% wt	0.09	0.31	0.41	0.014	0.005	0.016	8.56	0.26	0.92	0.21	0.065	0.042

The constitutive model developed is a multi-mechanisms model. Reference [8] describes it in details and presents the validation. For the undamaged material, three viscoplastic deformation mechanisms are considered following classical descriptions of creep flow mechanisms: the first one accounts for loading and final rupture stages (quasi plastic flow regime), the second one for viscoplastic creep regime (dislocation climb mechanism) and the third one for diffusional creep regime (grain boundary diffusion mechanism). An additive decomposition of the contribution of each mechanism is assumed. The total strain rate tensor is the sum of the different strain rate tensors.

A coupling between flow and damage is introduced. At each viscoplastic creep mechanism is associated a damage evolution, represented by the void volume fraction evolution: both nucleation of cavities and their growth by diffusion and by viscoplastic deformation of the matrix are considered. The effect of stress triaxiality is taken into account in nucleation rate. Finally, a coupling is assumed between the contributions of porosity given by each mechanism. It means that a cavity which has nucleated due to a given mechanism can grow under the effect of another mechanism.

The identification of this model for the BM at 625°C is presented in [8]. A simulation of tests on

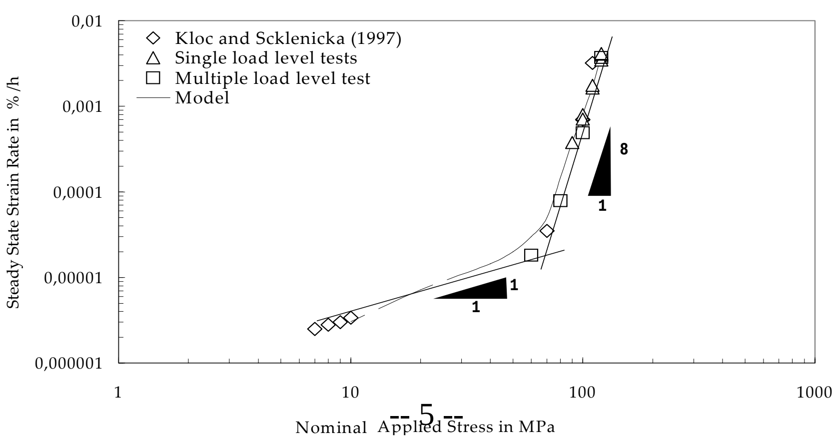

various samples was performed in order to validate it: smooth specimens, round U-notched bars with 2 different notch radii, round V-notched bars. Very satisfactory results were obtained. A good agreement is obtained between experimental and FE calculated creep curves for all kinds of samples. Figure 4 (from [8]) shows the prediction of the steady state strain rate obtained by the model, compared to experimental results in a wide range of stress level. On this figure, we clearly note the 2 different deformation mechanisms, with a transition around 70 MPa. Moreover a good prediction of the localization of damage and of the time to rupture on notched specimens is reached (fig. 5 from [8]).
Figure 4: steady state strain rate versus stress. Comparison of experimental results and model prediction

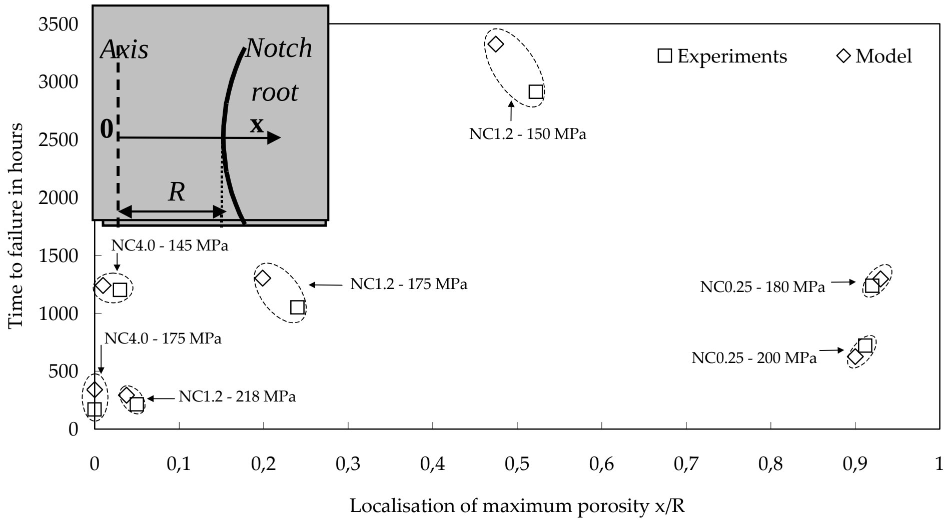

Figure 5: localisation of the most damaged zone at the onset of rupture for notched specimens. Comparisons between experimental observations and model predictions.

The ability of the model to represent experimental results at 600 and 650°C is proved in [8]. Further work would be necessary to validate its use to other temperature range. Work is also in progress to obtain the model identification for the HAZ. It will allow to calculate welded structures by considering the behavior and damage evolution of each zone: BM, HAZ and WM and to predict the life of such structures.

iii. Creep-fatigue behavior

First, some tests, including hold times or not, have been carried out at 550°C on the same 9Cr1Mo plate as the one used for fatigue studies. The aim was to check the stress-strain and damage behavior of this steel. No anomaly has been observed.

Second, a physically based study has been undertaken to simulate the cyclic softening of this steel. It should be noticed that tests including long hold times are impossible to carry out in laboratories. The in-service conditions correspond precisely to long hold times. Therefore, there is a need of simulations taking into account the physical mechanisms in order to propose reliable predictions and extrapolations corresponding to the in-service conditions. The study concerning cyclic softening is detailed in [9].

Several scales are involved in the microstructure of the martensitic 9Cr1Mo steel (Fig. 6a). First, blocks are about 4 μm, second laths inside a block are elongated and their thickness is about 0.7 μm and third subgrains along the laths are equiaxed and their diameter is about 0.7 μm. Between blocks, the misorientations can be high but the misorientations inside a block are smaller than 5°.

Low-cycle fatigue tests under strain control condition are carried out including various temperatures, strain levels and hold times. During cycling a significant softening is observed that is the stress range decreases cycle by cycle. Hysteresis stress-strain curve study shows that the softening is mainly due to the backstress (or kinematic stress or long-range athermal stress) decrease.

Transmission Electron Microscopy observations are carried out, on the initial condition, after cycling with or without hold time (Fig. 6 a), b) and c)), and after ageing. A large number of lath and subgrain boundaries disappear during cycling. Only low-angle boundaries seem to annihilate that is the block boundaries have not disappeared during lifetime. Ageing is not the driving force because the aged specimen microstructure is similar to the initial condition ones.

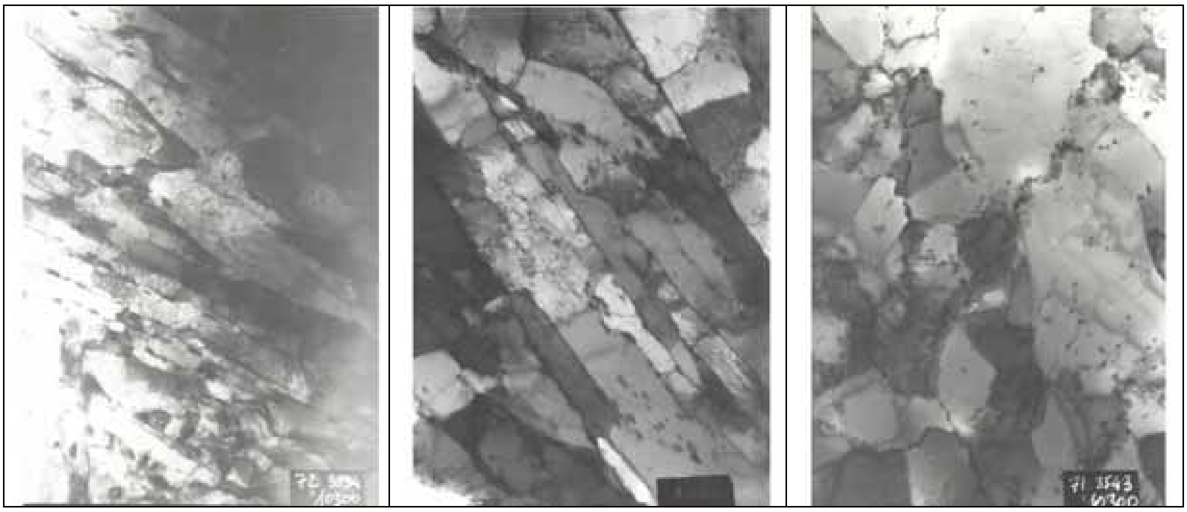

Figure 6: a) initial microstructure b) after cycling with no hold time c) after cycling with a hold time

Using these experimental data and observations, softening mechanism and modelling are proposed:

- mobile dislocations and dislocations of the low-angle boundaries (modelled as Read and Shockley tilt boundaries or similar boundaries) are supposed to interact (Fig. 7). If the distance between a mobile edge (screw) dislocation and a low-angle boundary edge (screw) dislocation of opposite sign is smaller than the edge (screw) annihilation distance, both dislocations annihilate. Because of cyclic slip and random cross-slip, the boundary dislocation densities and the misorientations are decreasing cycle by cycle.
- a part of the backstress is induced by a Hall-Petch type (grain size) effect. Following Li computation [16], the backstress corresponding to a tilt boundary depends on both the misorientation and grain size. In the calculation, the grain size is supposed to be associated to the smallest ones that is the sub-grain size.

Quantitative predictions of microstructure size and backstress cyclic evolutions are compared to the experimental results (Fig. 8).

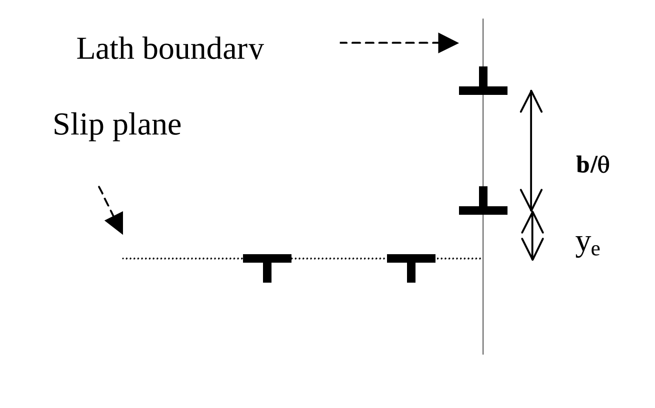

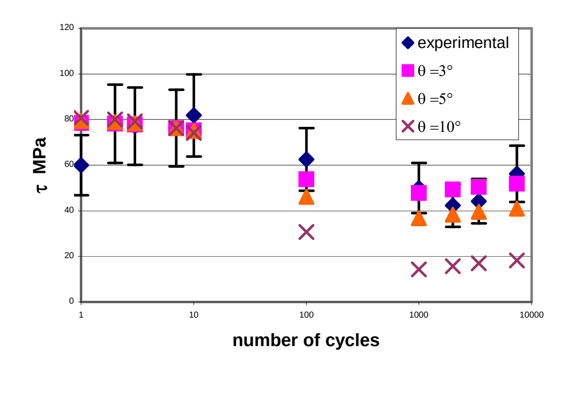

Fig. 7 : interaction between mobile dislocations and boundary dislocations
Fig. 8 : comparison between experimental and simulated backstresses (kinematic stress) (±0.3%). Three misorientations are considered.

Third, new creep-fatigue tests have been carried out, at 550°C, on this 9Cr1Mo steel, following previous work on 316LN stainless steel [10]. During the hold times, a constant stress level is applied, instead of a constant strain level as during a classical fatigue-relaxation test. Therefore, during the same total test, larger creep strains are reached than during the corresponding fatigue-relaxation test (as there is no stress relaxation during hold time). Such tests could help to predict the numbers of cycles to failure of fatigue relaxation tests with long hold times which can not be carried out in laboratories (1 month for example). These tests are in progress.

4. DEFECT NOCIVITY ASSESSMENT

High temperature defect assessment procedures under fatigue, creep and creep-fatigue loadings, have been developed for the fast reactors and have been mainly validated on austenitic stainless steels like 316L(N) [11, 15]. Concerning the GCR, complementary studies are conducted in order to validate the existing methods and to get new experimental data on 9%Cr martensitic steels. Moreover, if the geometry and the loading of a standard CT specimen allow to propose a 2D analysis, the case of industrial loadings appears much more complicated, notably because of surface defects which propagate and present shapes that can be considered as half ellipse. Therefore, in the frame of the defect assessment methods validation, the CEA realises both standard tests on CT specimens to determine the propagation laws and bending tests on large plates under high temperature fatigue, creep or creep-fatigue loadings. These components present an initial semi elliptical surface notch normal to the loading direction and its initiation and propagation are studied. Here, only the tests under fatigue are presented.

a) Experimental procedure

Material

The material of the study is the same as in fatigue and creep-fatigue studies. Each sample has been cut in order to be loaded in transverse direction and to make the crack propagate in the rolling direction.

Fatigue on CT specimens

The 25mm thick specimens are first fatigue pre-cracked at room temperature with a decreasing ΔK to a crack length of 27.5 mm (a/w=0.55). Then, they are side-grooved and their net thickness is 20mm. Fatigue tests on these standards CT specimens are realised according to ASTM E647 at 550°C, with a frequency of 0.1Hz and a load ratio R=0.1 in order to determine the Paris law. The crack length is followed by the compliance method and few points at the end of the test are rejected to ensure that the ligament length is sufficient to stay in a quasi-elastic domain all along the test. The Paris law obtained from 14 to 34 MPa.m$^{1/2}$ is given by equation 1.

$$\frac{da}{dN} = 7{,}1.10^{-7}\Delta K^{1.85} \qquad \text{Equation (1)}$$

$$(mm/cy) \quad (MPa.\sqrt{m})$$

Fatigue tests on P91 large plates

These tests on structures deal with large plate (590 mm × 440 mm × 30 mm) whose central width is reduced to 350 mm. A semi elliptical notch is machined in the plate center. The notch dimensions (depth (a) = 5 mm and width (2c) = 20 mm) have been chosen in order to be “isoK” : it means that, for our bending loading, the notch presents the same stress intensity factor K deeply and near the surface. First this plate is fatigue pre-cracked at room temperature with constant ΔF (Fmax=30 kN and R=0.1) and a frequency of 0.5Hz. A crack propagation of around 1mm all along the notch is obtained.

Then, the plate is submitted to cycling bending at 550°C. 60000 cycles are realised. The bending loading is obtained thanks to two arms of 352.5 mm long (figure 9). The heating is ensured by a radiant furnace fixed on the specimen in order to follow its displacements during the test and to obtain a very homogeneous temperature (± 3°C) on the central zone of the plate. The test is realised by imposing a constant ΔF (Fmax=47.1 kN and R=0.1).

Periodically beach-markings are realised under fatigue with a different R ratio in order to temporarily modify the propagation conditions. These are then visible to the naked eye on the rupture surface and constitute reference marks all along the test to determine the crack propagation.

Instrumentation is made up of 17 thermocouples to ensure an homogeneous temperature distribution. Moreover, the displacement and the load produced by the press are recorded. The arms rotation and the plate deflection f are followed to correct the moment effectively applied. Two laser micrometers allow to measure the crack opening displacement (CMOD) and the crack opening angle (α=CMOA). Finally, the crack propagation is also monitored using the potential drop method (PD) or the compliance method. More details on the instrumentation can be found in [14]

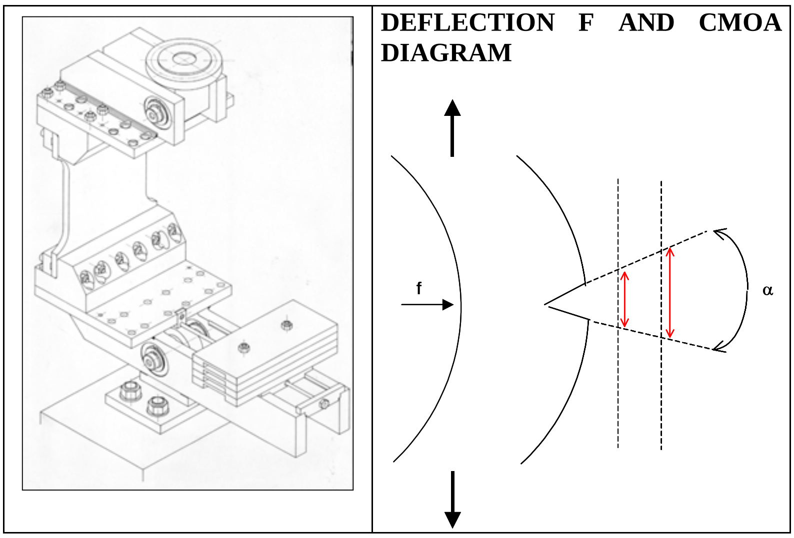

Figure 9 : principle of the fatigue test on large plates

b) Numerical calculations

In order to interpret these tests on structures, finite element calculations are necessary. They let to confirm the crack propagation by using the compliance, but also to calculate the global parameters of fracture mechanics K, J and C*.

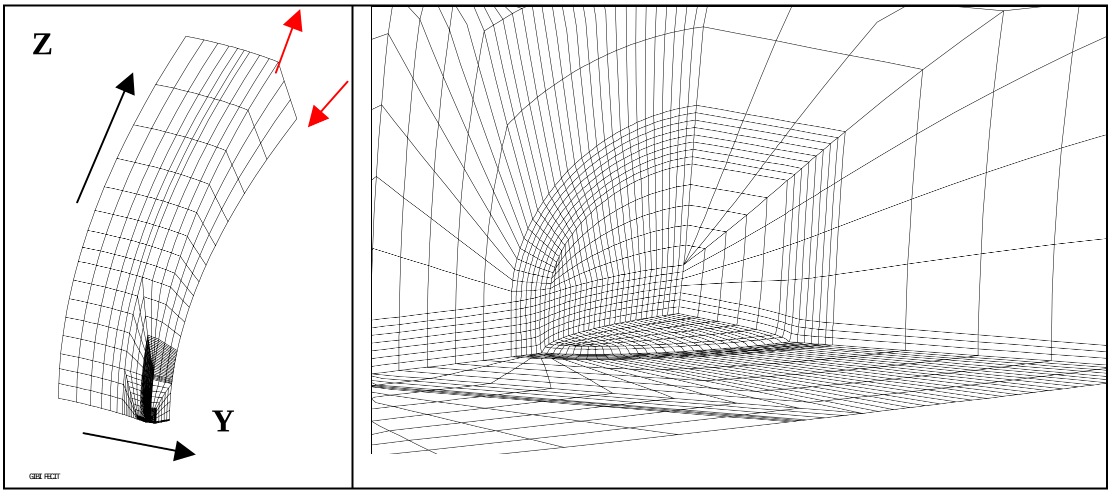

Figure 10 : Example of mesh used to interpret the tests on cracked plates

In this case, the aim of this calculation is more particularly to build the compliance function linking, for a bending moment, the opening angle (CMOA) to the propagation which is described by the couple (a, c) or (a, c/a). 21 finite element calculations are realised by considering 7 crack depths from 6.5 to 18 mm and 3 ratios c/a equals to 1.8, 2 or 2.2. These numerical analyses are based on 3D models (figure 10), representing a quarter of the plate in the zone where the temperature is homogeneous. The semi elliptical front is meshed in order to simulate accurately the experimental defects and the limit conditions allow to impose a pure bending moment. All the analysis are realised with massive quadratic elements by using the code CAST3M [12]. The mechanical behavior is supposed to be elastic with a Young modulus of 160 GPa and a Poisson coefficient of 0.3.

c) Principle of analysis and results

The first part of the analysis consists in observing the fracture surface. The initial semi elliptical crack keeps its shape all along the test, and its length/depth ratio (c/a) is between 1.8 and 2.2. For the known points, the evolution of the defect dimensions can be built as a function of potential drop or of the experimental CMOA, or of the numerical compliance. These points are the end of pre-cracking, the 3 beach-marking (realised after 15000 cycles, 25000 cycles and 43000 cycles) and the final defect. Either a linear correlation (PD1), or quadratic or cubic polynomial correlations (PD2 and PD3) can be used with the potential drop. A linear correlation is chosen to describe the link between the propagation and the experimental CMOA. And finally, the numerical compliance allows to consider that the numerical CMOA varies linearly with the crack depth (a) and that the result does not depend a lot on the ratio c/a between 1.8 and 2.2. Thanks to these calculations, for an experimental measurement of CMOA, the crack depth (a) and the crack length (2c) can be determined. The results of these five analyses are presented on figure 11. All these methods give similar results in very good agreement with the experimental data. This point constitutes an essential validation of all the involved measurements and of the many successive analysis.

Then, the second step of the analysis is to determine the propagation speed for the crack depth (a) and for the crack length in surface (2c). The mean speed during the i^{th} cycle is calculated according to equation 2.

$$\left(\frac{da}{dN}\right)_i = \frac{a_{i+1} - a_{i-1}}{N_{i+1} - N_{i-1}} \qquad \text{Equation (2)}$$

The third part of the analysis deals with the determination of the global parameter K. It has been done by using a specific K_I handbook [13].

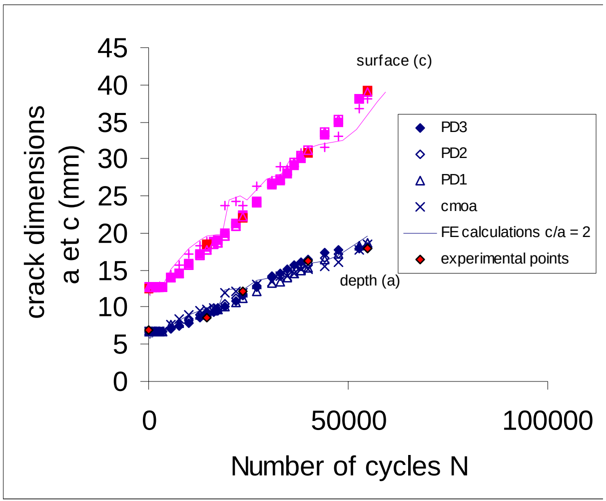

Fig. 11 : determination of the propagation by the five correlation types

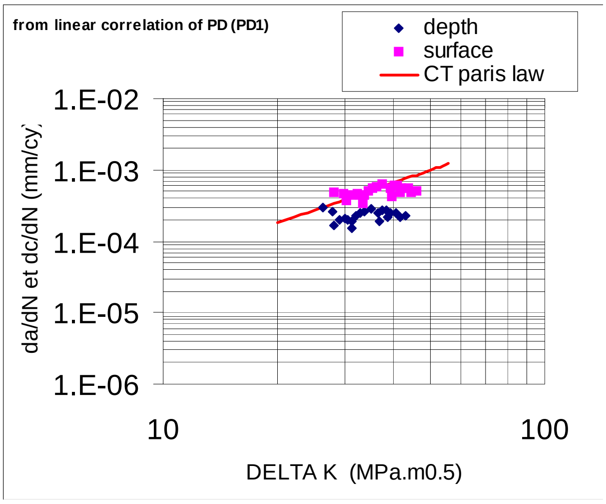

Fig. 12 : Propagation speed as a function of ΔK

Finally, a diagram showing the crack speed as a function of ΔK is presented on figure 12. By using the potential drop method, it is shown that the propagation speed is twice faster in surface than in depth. This could question the application of the Paris law, because for the same ΔK we do not reach the same speed. But, on the other hand, one reason could be a wrong estimation of ΔK in depth because we do not take into account any closure effect. This would reduce the ΔK and move the experimental points closer to the Paris law. Moreover, the Paris law can be applied correctly in surface, where no closure effect can occur. This emphasizes the idea that if the local loading is correctly estimated, the Paris law is able to describe the crack propagation in the plate.

5. CONCLUSIONS

A research program is undertaken on mod 9Cr-1Mo steel in order to improve the knowledge concerning the mechanical behavior in fatigue, creep and creep-fatigue situations for the base metal and for the welded junctions.

Traction-torsion tests allow to point out the influence of the mean tensile stress on the fatigue endurance. This effect appears to be enhanced in the case of low strain ranges, which corresponds to the in-service conditions. Complementary tests will be performed to investigate more precisely such conditions and to characterize the ratcheting behavior of the material.

A major point to validate the use of this steel for the pressure vessel will be the determination of the negligible creep domain. Important differences exist for creep strain laws at low temperatures and low stress levels between codified RCC-MR data and reference [6] which seems to be the base for the construction of isochronous curves of ASME. Specific studies are in progress at CEA to identify more precisely the creep strain laws in these loading conditions.

Specific studies are running to derive creep behavior and creep damage models which can be used with confidence for the prediction of the lifetime of the structures. These models are based on the physical mechanisms of deformation and of damage. An identification of these models at 625°C has been performed. It allows to obtain very satisfactory results, when compared to experimental results on different samples.

Creep-fatigue behavior is also studied. Tests in strain control conditions for different values of temperatures, strain levels and hold time have been performed. Metallurgical observations lead to propose physically based constitutive models, which compare favourably with experimental results. Moreover tests in creep-fatigue situations are realised: a constant stress level is maintained during hold times. Such tests allow to reach higher creep damages than in fatigue-relaxation tests, for lower hold times.

In order to validate high temperature defect assessment procedures for martensitic steels, the Paris law of Z10CDVNb9.1 steel has been determined at 550°C. Tests on cracked structures are realised. A fatigue test at 550°C on a semi elliptical notch is detailed. The crack propagation is followed by potential drop correlations, opening angle correlation and compliance method. Moreover, ΔK is calculated by using a specific handbook. It is shown that the crack propagation at the plate surface is correctly estimated by the Paris law because no closure effect can be involved there. On the other hand, this phenomena of closure is probably more pronounced for the deepest point, which may lead to an overestimation of the local loading and therefore to a wrong call into question of the Paris law.

All these studies are still running, and complementary results will be obtained in the next months.

ACKNOWLEDGEMENT

Research studies on creep behavior and creep damage evaluation for base metal and welded junctions are carried out in the framework of a PhD program involving EMP (Ecole des Mines de Paris), EDF, FRAMATOME-ANP and CEA.

REFERENCES

[1] P. Billot, J.L. Seran, M.T. Cabrillat, H. Burlet, A. Terlain, J.P.Bonal, CEA R&D Program on Structural Materials for the Very High temperature Reactor (VHTR), ANS/ENS Global 2003 meeting, New Orleans, November 2003

[2] J.L. Seran et al, Metallic and graphite materials for out-of core and in-core components of the VHTR: first results of the CEA R&D Program, HTR 2004, paper E15

[3] D. Buckthorpe et al, High Temperature Reactor Materials: Progress of HTR-M Projects, High Temperature Reactor Materials: Progress of HTR-M Projects, NEA/OECD, 3rd Information Exchange meeting on High Temperature Engineering, JAERI, Ibaraki-ken, Japan, 11-12 September 2003

[4] P. Billot et al, CEA R&D Program on Structural Materials for the Future Gas-Cooled Nuclear Systems, 3rd Information Exchange meeting on High Temperature Engineering, JAERI, Ibaraki-ken, Japan, 11-12 September 2003

[5] RCC-MR 2002, Design and Construction Rules for Mechanical components of FBR nuclear islands and high temperature applications, AFCEN, Edition 2002

[6] R.W. Swindeman, Construction of isochronous stress strain curves for 9Cr-1MoV steel, , PVP Vol 391, Advances in Life prediction methodology, ASME 1999

[7] B. Michel, Formulation of a new intergranular creep damage model for austenitic stainless steels, Nuclear Engineering and Design, 227, 2004, pp 161-174

[8] V. Gaffard, J. Besson, A.F. Gourgues, Creep failure Model of a 9Cr-1MoNbV (P91) steel integrating multiple deformation and damage mechanisms, ECF15, Stockholm, Sweden, August 2004.

[9] M. Sauzay, H. Brillet, I. Monnet, M. Mottot, A. Pineau, Cyclically induced softening due to low-angle boundary annihilation in a martensitic steel , Dislocations 2004 Congress, France, Sept. 2004.

[10] M. Mottot, M. Sauzay, M. Noblecourt, L. Allais, Nucl. Eng. Des., in the press, 2004

[11] Annex A16 of the RCC-MR code 2002.

[12] *http://www-cast3m.cea.fr/cast3m/index.jsp*

[13] S. Chapuliot, Formulaire de KI pour les tubes comportant un défaut de surface semi elliptique longitudinal ou circonférentiel interne ou externe, Rapport CEA-R-5900, 2000

[14] F. Curtit, Propagation de fissures semi-elliptiques en fatigue-Fluage à 650°C dans des plaques d'acier 316L(N) avec ou sans joints soudes, Thèse en sciences et génie des matériaux à l'Ecole Nationale Supérieure des Mines de Paris, 1999.

[15] B. Drubay, S. Marie, S. Chapuliot, M.H. Lacire, B. Michel, H. Deschanels, A16 : guide for defect assessment at elevated temperature, Int. Journal of Pressure Vessels and Piping, 80, 2003, pp.499-516

[16] J.C. M. Li, Trans TMS-AIME, 1963, vol 227, p. 239-247